

Point Defects in Pb-Doped Sb₂Te₃ Single Crystals

T. Plecháček and J. Horák

Joint Laboratory of Solid State Chemistry of the Academy of Sciences of the Czech Republic and University of Pardubice, Studentská 84, 532 10 Pardubice, Czech Republic

Received August 4, 1998; in revised form February 22, 1999; accepted February 26, 1999

Single crystals of Sb₂Te₃ doped with Pb atoms ($c_{\text{Pb}} = 0\text{--}2.1 \times 10^{20}$ atoms/cm³) were characterized by the measurements of the reflectivity in the plasma resonance frequency region, the Hall coefficient, the electrical conductivity, and the Seebeck coefficient. Measurements of the Hall coefficient for a series of Pb-doped Sb₂Te₃ crystals served to determine the concentration of holes as a function of the Pb content in the lattice. The obtained variation of the hole concentration is ascribed to the formation of substitutional defects Pb_{Sb} and to the interaction of the Pb atoms entering into the lattice with anti-site defects and vacancies in the tellurium sublattice. Improved ideas on point defects in the Pb-doped Sb₂Te₃ single crystals are formulated in this paper. © 1999 Academic Press

Key Words: crystals of tetradymite structure; Hall coefficient; electrical conductivity; Seebeck coefficient; reflectivity in the plasma resonance frequency region, lattice defects.

INTRODUCTION

Sb₂Te₃ crystals rank among the family of layered narrow-gap semiconductors of tetradymite structure (space group $D_{3d}^5\text{--}R\bar{3}m$). The lattice of trigonal Sb₂Te₃ crystal consists of layers, each layer comprising five atomic planes oriented perpendicular to the trigonal *c*-axis and alternating according to the scheme:



There is a van der Waals gap between the Te¹ atomic planes.

Due to the applications of both undoped and doped Sb₂Te₃ crystals in the field of thermoelectric devices (1), research of physical and chemical properties of these materials is of great importance. Except the monocrystalline material, attention is devoted to the study of thin films (2) and surface phenomena (3).

The Sb₂Te₃ crystals prepared from the melt of stoichiometric composition 2Sb/3Te exhibit always a surplus of Sb (4), because tellurium partially segregates during growth. The overstoichiometric Sb atoms occupy

prevalingly the Te² sites in the tellurium sublattice and thus give rise to anti-site (AS) defects of the Sb_{Te}¹ type, carrying one negative charge (5), which is compensated by a hole. Because of thermoelectric applications, it is important to change, i.e., increase or decrease, the hole concentration by means of doping with suitable admixture. Many papers deal with the problem of doping atoms' incorporation into the structure of Sb₂Te₃ crystals and with the study of relevant changes of the electrical and thermoelectric properties. The influence of Pb atoms entering the crystal lattice on the transport coefficients was presented in (6, 7). In Ref. (6) the decrease of hole concentration in the region of low content of Pb atoms is declared; this decrease is in (7) explained by an "approach" to the stoichiometry. Investigation of the relations between lead atoms content in Sb₂Te₃ single crystals and some physical properties was done in (8). However, the opinion on the process of Pb atoms incorporation into the Sb₂Te₃ crystal structure has not been presented yet. In this article we present the results of our measurements of the Hall coefficient, the electrical conductivity, the Seebeck coefficient and the reflectivity in the plasma resonance frequency region and their dependencies on Pb content in the samples. On the basis of the hole concentration changes due to the lead doping we propose a qualitative model; we consider not only the rise of the substitutional defects in the cation sublattice but also the interaction of Pb atoms with the native defects in Sb₂Te₃.

2. EXPERIMENTAL

2.1. Growth of Pb-Doped Sb₂Te₃ Single Crystals

The starting polycrystalline material was prepared from Sb, Te, and Pb of 5N purity. PbTe, prepared as the first compound, was used for doping. The final syntheses were carried out in evacuated conical silica ampoules where PbTe was added to the stoichiometric mixture of Sb and Te, corresponding to the Sb₂Te₃ composition; the reaction mixture was heated at 1073 K for 48 hours. The growth of the single crystals was carried out in the same ampoules by means of a modified Bridgman method (9, 10) using a

suitable temperature gradient 80 K/cm and a pulling rate of 1.3 mm/h.

The obtained single crystals, 50 mm in length and 10 mm in diameter, could be easily cleaved. Their trigonal axis c was always perpendicular to the pulling direction so that the (0001) plane was parallel to the ampoule axis. The orientation of the cleavage faces was carried out using the Laue back-diffraction technique, which confirmed that these faces were always (0001).

The samples were cut out from the central part of the single crystals. First the reflectivity was measured on the natural cleavage faces and then the measurement of the Hall coefficient, the electrical conductivity, and the Seebeck coefficient were carried out. Finally, the actual concentration of lead c_{Pb} in these samples was determined using atomic absorption spectrometry.

2.2. Measurements of the Transport Coefficients and the Seebeck Coefficient

The electrical conductivity σ and the Hall coefficient R_{H} were measured on the bar samples of dimensions $14 \times 3.5 \times (0.1-0.3) \text{ mm}^3$ in the temperature range from 90 to 420 K. The measurements were realized using alternating current at a frequency of 1020 Hz. A stationary magnetic field having a induction $B = 0.7 \text{ T}$ and an orientation $B \parallel c$ was used. The current contacts were made with the help of coated gold layer and silver paste; mechanical contacts for the Hall voltage measurement were used. The value of the electrical conductivity $\sigma_{\perp c} \equiv \sigma$ has been determined from

the potential drop across the sample between the voltage contacts. All temperature dependencies were measured in the linear heating regime at the rate of 1 K per minute.

The Seebeck coefficient $\alpha_{\Delta T \perp c} \equiv \alpha_{\text{k}}$ was measured in the temperature range of 150–450 K; the sample orientation with respect to the temperature gradient always fulfilled the condition $c \perp \Delta T$. The temperature difference ΔT between the cold and hot junction did not exceed 10 K.

2.3. Measurements of the Reflectivity Spectra

Special dependencies of the reflectivity in the plasma resonance frequency were measured at room temperature in unpolarized light on natural (0001) cleavage planes using a Biorad FTS-45 FT-IR spectrometer with a specular reflectance accessory. The geometry of the experiment was such that the electric field vector E of the electromagnetic radiation was always perpendicular to the trigonal c -axis, i.e., $E \perp c$. For the recording of the spectrum the following procedure was used. First the background single beam spectrum was collected by using an aluminum mirror in place of the sample, then the sample single beam was recorded and the reflectivity spectrum was obtained as the ratio of the sample to background spectrum. In this way the reflectivity spectra in the wavenumbers region $600-2600 \text{ cm}^{-1}$ were obtained.

3. DISCUSSION

The results of the measurement of reflectivity R in the plasma resonance frequency are shown in Fig. 1. It is

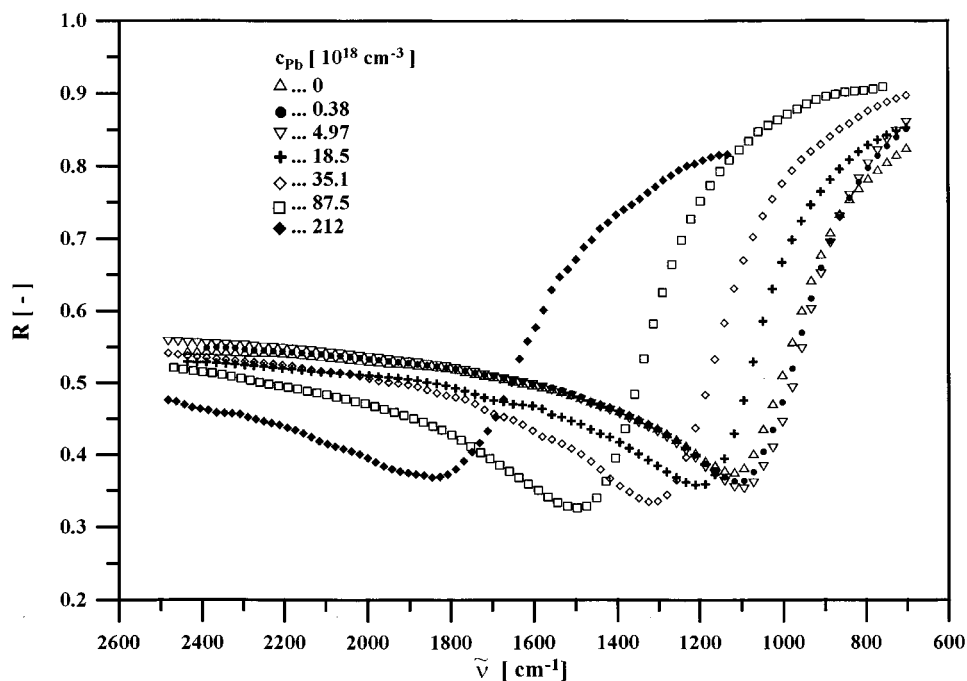


FIG. 1. Reflectivity spectra of Pb-doped Sb_2Te_3 single crystals.

TABLE 1
Optical Parameters of Pb-Doped Sb_2Te_3 Single Crystals

| Sample no. | c_{Pb} [cm ⁻³] | $\tilde{\nu}_{\text{min}}$ [cm ⁻¹] | ε_{∞} [-] | τ [10 ⁻¹⁴ s] | ω_{p} [10 ⁻¹⁴ s] | p/m_{\perp} [10 ²⁰ cm ⁻³] |
|------------|-------------------------------------|--|----------------------------|------------------------------|---|--|
| 1 | 0 | 1124 | 56.0 | 2.0 | 1.97 | 6.84 |
| 2 | 3.80×10^{17} | 1113 | 55.7 | 2.2 | 1.94 | 6.57 |
| 3 | 4.97×10^{18} | 1090 | 55.5 | 2.4 | 1.92 | 6.42 |
| 4 | 1.85×10^{19} | 1200 | 55.5 | 2.2 | 2.13 | 7.91 |
| 5 | 3.51×10^{19} | 1319 | 55.1 | 2.2 | 2.32 | 9.28 |
| 6 | 8.75×10^{19} | 1491 | 55.1 | 2.1 | 2.65 | 12.2 |
| 7 | 2.12×10^{20} | 1846 | 55.0 | 1.3 | 3.25 | 18.2 |

evident that the reflectivity spectra exhibit a pronounced minimum. The location $\tilde{\nu}_{\text{min}}$ of the individual samples minimum (see Table 1) implies that the incorporation of Pb atoms into the Sb_2Te_3 crystal lattice causes a shift of the reflectance minima toward lower wavenumbers in the range of low Pb concentration ($c_{\text{Pb}} < 5 \times 10^{18} \text{ cm}^{-3}$). The reflectance minima of the samples with higher Pb content are, on the contrary, situated at higher wavenumbers, as compared to the location of the minimum for undoped Sb_2Te_3 . This effect is undoubtedly associated with the variation of hole concentration and consequently with the concentration of point defects. In order to obtain information on the changes in the free carrier concentration, associated with an incorporation of Pb into the Sb_2Te_3 lattice, the experimental $R = f(\tilde{\nu})$ curves were fitted using equations for the real and imaginary parts of the complex dielectric function following from the Drude-Zener theory (11). From the values of the plasma resonance frequency ω_{p} obtained in this way, the values of the p/m_{\perp} ratio, using the relation valid for the presence of a single type of free charge carriers (holes)

$$\omega_{\text{p}} = \left(\frac{p \cdot e^2}{\varepsilon_0 \varepsilon_{\infty} m_{\perp}^*} \right)^{1/2}, \quad [1]$$

were calculated (p is the hole concentration, e is an elementary charge, ε_0 is the permittivity of free space, ε_{∞} is the high-frequency relative permittivity, and $m_{\perp} m_0$ the free carrier effective mass). The results of this analysis are summarized in Table 1. Taking, in the first approximation, the effective mass value m_{\perp} for a constant, we can conclude that the hole concentration presents a minimum near the dopant content $c_{\text{Pb}} \cong 5 \times 10^{18} \text{ atoms/cm}^3$.

In Figs. 2 to 4, the temperature dependencies of transport parameters (Hall coefficient, electrical conductivity, Seebeck coefficient) for several Pb atoms' content, i.e., $R_{\text{H}} = f(T, c_{\text{Pb}})$, $\sigma = f(T, c_{\text{Pb}})$, and $\alpha_{\text{k}} = f(T, c_{\text{Pb}})$, are illustrated. They verify the presence of a minimum of the hole concentration, following from the interpretation of the reflectivity

spectra. This result is qualitatively in agreement with the statement in Ref. (6).

To explain this anomalous effect, i.e., the minimum in $p(c_{\text{Pb}})$ dependence, the hole concentration p and its changes Δp were calculated from the experimental Hall coefficient values R_{H} at room temperature. The relation $R_{\text{H}} = \gamma \cdot r_{\text{H}}/p \cdot e$ was used, where r_{H} is the Hall factor, γ is the anisotropy factor, and e is the elementary charge. In view of the fact that the band structure of Pb-doped Sb_2Te_3 is not well known, the calculations were performed with the value of $\gamma = 0.74$ published for Sb_2Te_3 (12). Thus, a simplification that the γ value is independent on c_{Pb} was adopted. Further, it was assumed that, given the relatively high concentration of the free charge carriers, the value of r_{H} is equal to unity. The hole concentration changes Δp were then calculated using the relation

$$\Delta p = \frac{\gamma}{e \cdot R_{\text{H}}(c_{\text{Pb}})} - \frac{\gamma}{e \cdot R_{\text{H}}(c_{\text{Pb}} = 0)}, \quad [2]$$

where $R_{\text{H}}(c_{\text{Pb}})$ is the Hall coefficient for the Pb-doped samples and $R_{\text{H}}(c_{\text{Pb}} = 0)$ is that for undoped Sb_2Te_3 . The results are summarized in Table 2 and illustrated in Fig. 5. The values $\Delta p/\Delta c_{\text{Pb}}$ in Table 2 are presented only for samples

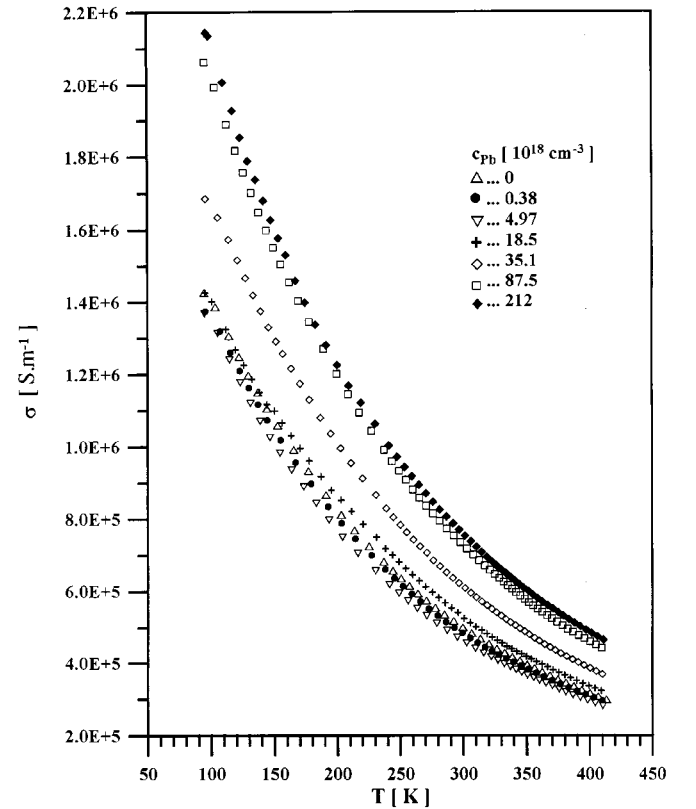


FIG. 2. Temperature dependencies of the Hall coefficient in Pb-doped Sb_2Te_3 crystals.

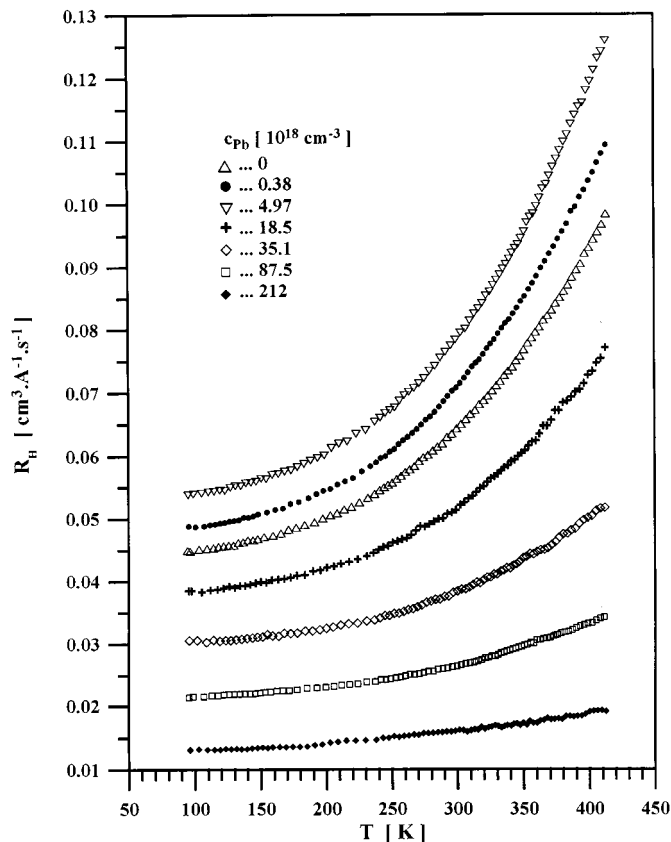


FIG. 3. Temperature dependencies of electrical conductivity in Pb-doped Sb_2Te_3 crystals.

with Pb content ($c_{\text{Pb}} > 1 \times 10^{18} \text{ cm}^{-3}$), where the error of the value is smaller than $\pm 10\%$.

The increase of the hole concentration in the region of lead content $1.3 \times 10^{19} < c_{\text{Pb}} < 2 \times 10^{20} \text{ atoms/cm}^3$ can be qualitatively explained; Pb atoms substitute the sites in antimony sublattice, forming Pb'_{Sb} substitutional defect with one negative charge, which is compensated by a hole h^{\cdot} . To explain variation of hole concentration for $c_{\text{Pb}} < 1.3 \times 10^{19} \text{ atoms/cm}^3$ we propose a qualitative model based on ideas of interaction of Pb atoms with the native defects in Sb_2Te_3 . Due to the superstoichiometry of Sb, which arises during the growth of Sb_2Te_3 , the following point or structural defects can be taken into account:

(1) $V_{\text{Te}}^{\cdot\cdot}$ vacancy in the tellurium sublattice. In this model we ascribe two negative charges to this defect at room temperature. A defect of this type is also considered in the isostructural Bi_2Te_3 crystal (13, 14).

(2) Negatively charged Sb'_{Te} AS defects arise by entering the Sb atom into the Te sublattice.

(3) Structural defects of “seven-” or “nine-layer lamellae” Sb_3Te_4^- , resp. $\text{Sb}_4\text{Te}_5^{-2}$. The existence of these defects can be expected according to Refs. (15, 16).

However, the defects mentioned in (2) and (3) are indistinguishable by means of the hole concentration measurement or chemical analysis and so we assume the interaction of Pb atoms with AS defects. Further, we adopt the following principles and simplifications:

(a) The native defects arise during the crystal growth, i.e., on transition from the melt into the solid phase (melting point T_m); on further cooling their concentration can vary, remaining constant below a certain temperature T_x . This is acceptable in view of the fact that the formation energy of the defects is higher than $k_B T_x$ (k_B is the Boltzmann constant). We use the simplification $T_x = T_m$.

(b) The interaction between Pb atoms, entering into the crystal lattice, and native defects passes at T_m . Below this temperature, concentration of point defects is unchanged.

(c) The process of the creation and interaction of the native defects approaches the equilibrium state, which we formulate by means of the equation

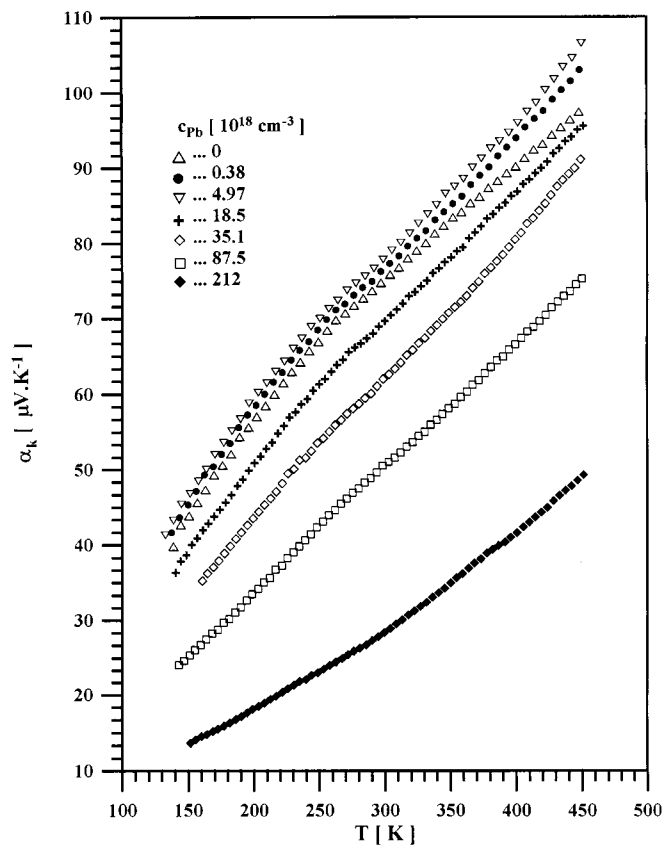
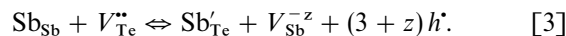


FIG. 4. Temperature dependencies of Seebeck coefficient in Pb-doped Sb_2Te_3 crystals.

TABLE 2
Hole Concentration p and Its Changes Δp in Pb-Doped Sb₂Te₃ Single Crystals

| Sample no. | c_{Pb} [cm ⁻³] | p_{exp} [cm ⁻³] | Δp [cm ⁻³] | $\Delta p/\Delta c_{\text{Pb}}$ [-] |
|------------|--|---|-----------------------------------|--|
| 1 | 0 | 7.64×10^{19} | 0 | 0 |
| 2 | 1.9×10^{17} | 7.78×10^{19} | 1.37×10^{18} | - |
| 3 | 3.7×10^{17} | 7.13×10^{19} | -5.08×10^{18} | - |
| 4 | 3.8×10^{17} | 6.93×10^{19} | -7.08×10^{18} | - |
| 5 | 3.9×10^{17} | 6.41×10^{19} | -1.23×10^{19} | - |
| 6 | 9.6×10^{17} | 6.77×10^{19} | -8.69×10^{18} | - |
| 7 | 2.80×10^{18} | 6.48×10^{19} | -1.16×10^{19} | -4.1 |
| 8 | 2.86×10^{18} | 6.63×10^{19} | -1.01×10^{19} | -3.5 |
| 9 | 2.89×10^{18} | 6.43×10^{19} | -1.21×10^{19} | -4.2 |
| 10 | 4.97×10^{18} | 6.26×10^{19} | -1.38×10^{19} | -2.8 |
| 11 | 1.32×10^{19} | 7.28×10^{19} | -3.62×10^{18} | -0.3 |
| 12 | 1.41×10^{19} | 8.09×10^{19} | 4.47×10^{18} | 0.3 |
| 13 | 1.76×10^{19} | 9.16×10^{19} | 1.53×10^{19} | 0.9 |
| 14 | 1.85×10^{19} | 9.47×10^{19} | 1.83×10^{19} | 1.0 |
| 15 | 3.51×10^{19} | 1.27×10^{20} | 5.07×10^{19} | 1.4 |
| 16 | 4.11×10^{19} | 1.35×10^{20} | 5.84×10^{19} | 1.4 |
| 17 | 4.35×10^{19} | 1.32×10^{20} | 5.61×10^{19} | 1.3 |
| 18 | 8.75×10^{19} | 1.82×10^{20} | 1.06×10^{20} | 1.2 |
| 19 | 2.12×10^{20} | 3.03×10^{20} | 2.26×10^{20} | 1.0 |

Introduction of the admixture to the melt disturbed the equilibrium and caused changes in the concentration of defects and free current carriers.

(d) As the crystal prepared from the melt of stoichiometric composition possesses superstoichiometry of Sb and high content of AS defects, we suppose that

$$[V_{\text{Sb}}^{-z}] \ll [V_{\text{Te}}^{+z}], \quad [V_{\text{Sb}}^{-z}] \ll [\text{Sb}'_{\text{Te}}] \quad [4]$$

At given conditions we can express the concentration of holes, AS defects, and vacancies at room temperature by the relations

$$p = [\text{Sb}'_{\text{Te}}] - 2[V_{\text{Te}}^{+z}] + [\text{Pb}'_{\text{Sb}}] \quad [5]$$

$$[\text{Sb}'_{\text{Te}}] = k_1/2 [\text{Sb}_{\text{Sb}}] \exp(-E_{\text{AS}}/k_{\text{B}}T_{\text{m}}) \quad [6]$$

$$[V_{\text{Te}}^{+z}] = [\text{Te}_{\text{Te}}] \exp(-E_{\text{V}}/k_{\text{B}}T_{\text{m}}), \quad [7]$$

where k_1 is a statistical factor referring to the formation of a single AS defect in the tetradymite crystal; irrespective of energy considerations it takes on a value of 1.2 (17). $[\text{Sb}_{\text{Sb}}]$ and $[\text{Te}_{\text{Te}}]$ are the numbers of Sb and Te sites per 1 cm³, E_{AS} and E_{V} are the energies of formation of AS defects and vacancies V_{Te}^{+z} , respectively, k_{B} is the Boltzmann constant, and T_{m} is the melting point temperature.

Lead atoms entering into the Sb₂Te₃ crystal give rise to the Pb'_{Sb} substitutional defects; the polarity of Pb'_{Sb}-Te²⁻ or

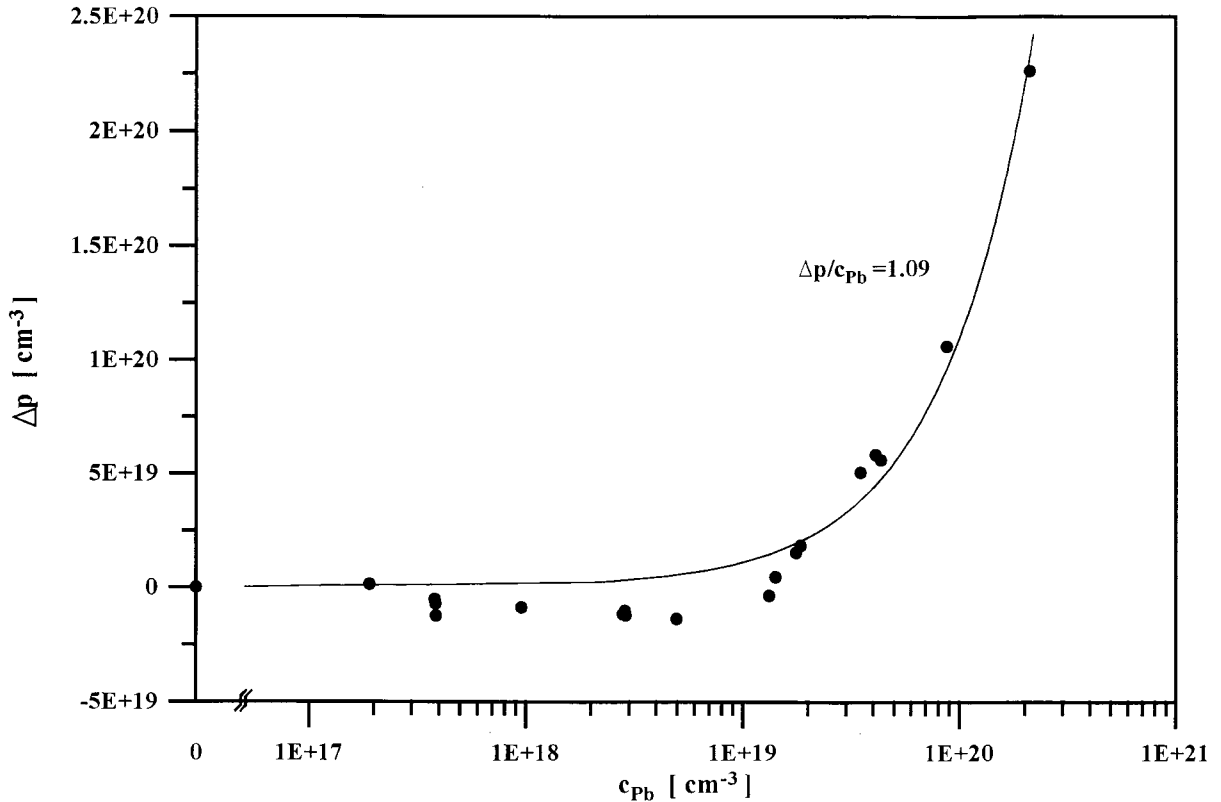


FIG. 5. Dependence of the hole concentration changes Δp on Pb-atoms' content in Pb-doped Sb₂Te₃ single crystals.

$\text{Pb}'_{\text{Sb}}\text{-Te}^1$ bonds increases, and thus the formation energy of the AS defect also increases; i.e., the energy required to move a Sb atom into a Te^2 site increases. This increase of formation energy ΔE_{AS} depends on the concentration of Pb atoms c_{Pb} ; in the first approximation the linear relation $\Delta E_{\text{AS}} = k_{\text{AS}}c_{\text{Pb}}$ is assumed. In the same way, the formation energy of tellurium vacancies is changed, too; i.e., $\Delta E_{\text{V}} = k_{\text{V}}c_{\text{Pb}}$. In a Pb-doped Sb_2Te_3 crystal we can express the concentration of holes ($[h'] \equiv p$) at room temperature by means of a relation:

$$p = \frac{1}{2} \cdot k_1 ([\text{Sb}_{\text{Sb}}] - [\text{Pb}'_{\text{Sb}}]) \cdot \exp\left[-\frac{E_{\text{AS}} + \Delta E_{\text{AS}}}{k_{\text{B}}T_{\text{m}}}\right] + [\text{Pb}'_{\text{Sb}}] - 2 \cdot [\text{Te}_{\text{Te}}] \cdot \exp\left[-\frac{E_{\text{V}} + \Delta E_{\text{V}}}{k_{\text{B}}T_{\text{m}}}\right]. \quad [8]$$

Experimentally determined dependence $p = f(c_{\text{Pb}})$ was fitted using Eq. [8] and the value $E_{\text{AS}} = 0.35$ eV according to Ref. (18). The obtained values of the concentration of AS defects, and of the tellurium vacancies, of the formation energies E_{AS} , E_{V} and their changes are presented in Table 3. It is evident from these results that in a consequence with qualitative ideas mentioned above the Pb atom incorporation causes a decrease of AS defects' concentration. It corresponds to the increase of formation energy E_{AS} from 0.35 eV for an undoped sample to 0.577 eV for the crystal with the highest Pb content (about 2×10^{20} atoms/cm³).

The concentration of vacancies is substantially reduced from the value of 5.1×10^{18} cm⁻³ about more than a factor of ten. These results confirm the ideas on the "approach to stoichiometry" due to the Pb atoms' incorporation formulated in Ref. (6).

On the base of approximate calculation of the concentration changes of point defects in crystals with various Pb content we can bring up the following conclusion: an increase of hole concentration is connected with a formation of Pb'_{Sb} substitutional defects and with a parallel decrease of the concentration of tellurium vacancie. It can be described by



where one incorporated Pb atom produces one hole. This is valid for $c_{\text{Pb}} > 1.7 \times 10^{19}$ atoms/cm³, as it is evident from the dependence of the ratio $\Delta p/\Delta c_{\text{Pb}}$ on lead content (see Table 2). In the region of low Pb content, the ratio is smaller than unity or even negative. It can be explained by a shift of the equilibrium expressed in Eq. [3] to the left. In our opinion this processes is connected with the bond polarity increase, a small drop of AS defect concentration, and a decrease of hole concentration. The mentioned relations are plotted in Fig. 6. Curve 1 shows the decrease of the concentration of AS defects, curve 2 shows the decrease of the concentration of holes compensating the charge of the vacancies V''_{Te} , and curve 3 shows the increase of the concentration of Pb'_{Sb} substitutional defects. Curve 4 represents the

TABLE 3
Hole Concentration, Calculated Concentration of Sb'_{Te} (AS) Defects and V''_{Te} Vacancies, and the Formation Energies E_{AS} and E_{V} in Pb-Doped Sb_2Te_3 Single Crystals

| Pb content [cm ⁻³] | p_{exp} [cm ⁻³] | p_{fit} [cm ⁻³] | $[\text{Sb}'_{\text{Te}}]$ [cm ⁻³] | $[V''_{\text{Te}}]$ [cm ⁻³] | E_{AS} [eV] | E_{V} [eV] |
|-----------------------------------|---|---|---|--|-------------------------|------------------------|
| 0 | 7.64×10^{19} | 7.45×10^{19} | 7.95×10^{19} | 5.10×10^{18} | 0.350 | 0.686 |
| 1.9×10^{17} | 7.78×10^{19} | 7.45×10^{19} | 7.94×10^{19} | 5.08×10^{18} | 0.350 | 0.686 |
| 3.7×10^{17} | 6.93×10^{19} | 7.46×10^{19} | 7.92×10^{19} | 5.07×10^{18} | 0.350 | 0.686 |
| 3.8×10^{17} | 6.41×10^{19} | 7.46×10^{19} | 7.92×10^{19} | 5.07×10^{18} | 0.350 | 0.686 |
| 3.9×10^{17} | 7.13×10^{19} | 7.46×10^{19} | 7.92×10^{19} | 5.07×10^{18} | 0.350 | 0.686 |
| 9.6×10^{17} | 6.77×10^{19} | 7.48×10^{19} | 7.85×10^{19} | 5.01×10^{18} | 0.351 | 0.687 |
| 2.80×10^{18} | 6.63×10^{19} | 7.55×10^{19} | 7.65×10^{19} | 4.85×10^{18} | 0.353 | 0.689 |
| 2.86×10^{18} | 6.48×10^{19} | 7.55×10^{19} | 7.65×10^{19} | 4.84×10^{18} | 0.353 | 0.690 |
| 2.89×10^{18} | 6.43×10^{19} | 7.56×10^{19} | 7.63×10^{19} | 4.83×10^{18} | 0.353 | 0.690 |
| 4.97×10^{18} | 6.26×10^{19} | 7.63×10^{19} | 7.43×10^{19} | 4.66×10^{18} | 0.355 | 0.692 |
| 1.32×10^{19} | 7.28×10^{19} | 8.01×10^{19} | 6.62×10^{19} | 4.01×10^{18} | 0.364 | 0.704 |
| 1.41×10^{19} | 8.09×10^{19} | 8.05×10^{19} | 6.54×10^{19} | 3.95×10^{18} | 0.365 | 0.705 |
| 1.76×10^{19} | 9.16×10^{19} | 8.24×10^{19} | 6.23×10^{19} | 3.70×10^{18} | 0.369 | 0.710 |
| 1.85×10^{19} | 9.47×10^{19} | 8.29×10^{19} | 6.15×10^{19} | 3.64×10^{18} | 0.370 | 0.711 |
| 3.51×10^{19} | 1.27×10^{20} | 9.37×10^{19} | 4.89×10^{19} | 2.69×10^{18} | 0.388 | 0.735 |
| 4.11×10^{19} | 1.35×10^{20} | 9.82×10^{19} | 4.50×10^{19} | 2.42×10^{18} | 0.394 | 0.743 |
| 4.35×10^{19} | 1.32×10^{20} | 1.01×10^{20} | 4.35×10^{19} | 2.31×10^{18} | 0.397 | 0.746 |
| 8.75×10^{19} | 1.82×10^{20} | 1.41×10^{20} | 2.36×10^{19} | 1.04×10^{18} | 0.444 | 0.808 |
| 2.12×10^{20} | 3.03×10^{20} | 2.92×10^{20} | 4.18×10^{18} | 1.08×10^{17} | 0.577 | 0.982 |

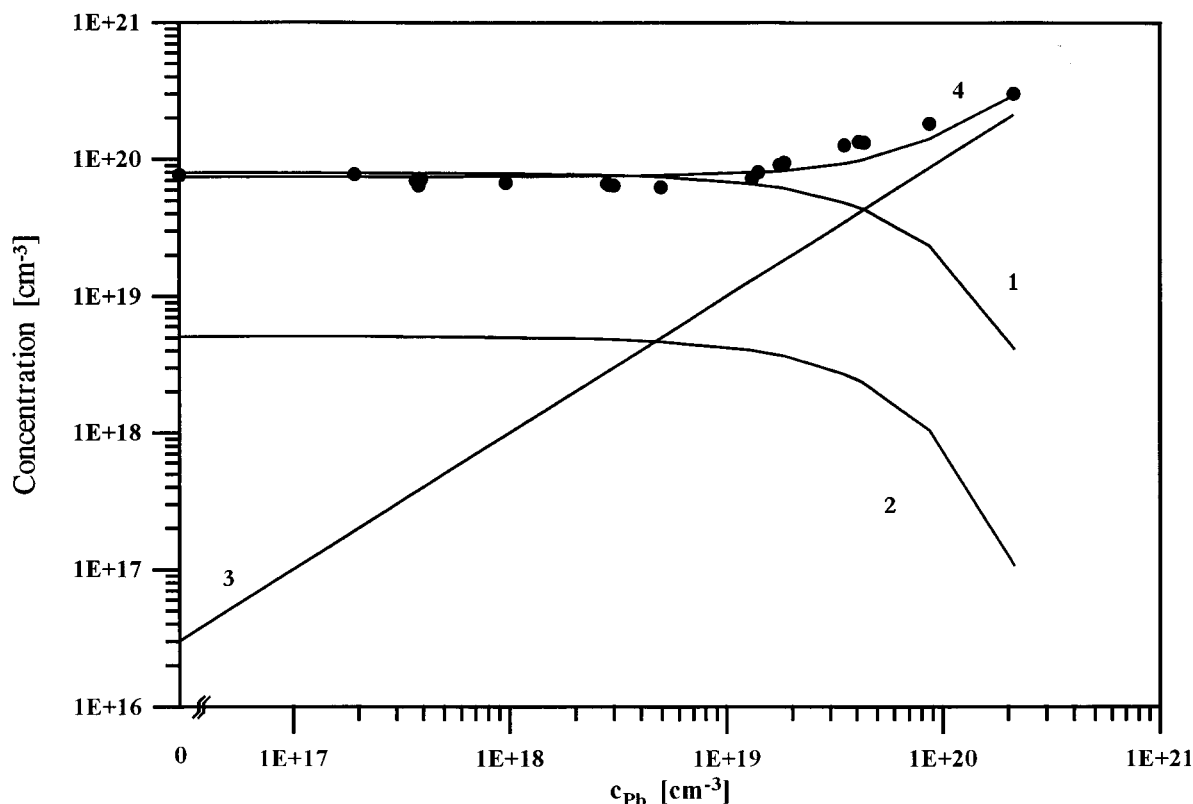


FIG. 6. Calculated concentration of AS defects (curve 1), concentration of free carriers compensating the charge of doubly charged $V_{\text{Te}}^{\bullet\bullet}$ vacancies (curve 2), concentration of the $\text{Pb}_{\text{Sb}}^{\text{B}}$ substitutional defects (curve 3), and hole concentration fitted using Eq. [8] (curve 4) as a function of the Pb-atoms' content in Pb-doped Sb_2Te_3 .

calculated hole concentration according to Eq. [8]. The full circles denote experimentally determined hole concentration.

The results obtained from the analysis of the course of $p = f(c_{\text{Pb}})$ dependence bring about the qualitative conclusions:

- The Pb atoms enter into the sites in antimony sublattice of Sb_2Te_3 single crystals forming the substitutional defects.

- The interaction between lead atoms and native defects, especially anti-site defects, takes place.

Finally, we compare published ideas of the entering of the Pb atoms into the Sb_2Te_3 and Bi_2Te_3 crystals. On the basis of theoretical considerations in Refs. (8, 13, 14) the authors assume that Pb atoms may occupy the Te sites in the tellurium sublattice of Bi_2Te_3 crystals. According to our result the idea of similar incorporation of Pb into the Te^1 or Te^2 sites in isostructural Sb_2Te_3 crystal seems to be improbable.

REFERENCES

1. H. Scherer and S. Scherer, "CRC Handbook of Thermoelectrics" (D. M. Rowe, Ed.), p. 211. CRC Press, Boca Raton, FL, 1995.
2. L. S. El Mandouh, *J. Mater. Sci.* **30**, 1273 (1995).
3. M. M. Ibrahim, *Appl. Phys. A* **52**, 237 (1991).
4. N. Kh. Abrikosov, L. V. Poretskaya, and I. P. Ivanova, *Zh. Neorg. Khim.* **4**, 2525 (1959).
5. J. Horák, S. Karamazov, P. Nesládek, and P. Lošťák, *J. Solid State Chem.* **129**, 92 (1997).
6. B. Rönnlund, O. Beckman, and H. Levy, *J. Phys. Chem. Solids* **26**, 1281 (1965).
7. F. Hulliger, "Structural Chemistry of Layer Type Phases" (F. Lévy, Ed.), p. 199. D. Riedel Dordrecht, 1976.
8. H. Süßmann, A. Priemuth, and U. Pröhl, *Phys. Status Solidi A* **82**, 561 (1984).
9. P. Lošťák, R. Novotný, L. Beneš, and S. Civiš, *J. Cryst. Growth* **94**, 656 (1989).
10. J. Navrátil, P. Lošťák, and J. Horák, *Cryst. Res. Technol.* **26**, 675 (1991).
11. O. Madelung, "Handbuch der Physik" (S. Flügge, Ed.), Vol. XX, p. 210. Springer-Verlag, Berlin, 1957.
12. M. Stordeur and G. Simon, *Phys. Status Solidi B* **124**, 799 (1984).
13. P. Pecheur and G. Toussaint, "8th Int. Conf. on Thermoelectric Energy Conversion, Nancy, France, 1989."
14. P. Pecheur and G. Toussaint, *J. Phys. Chem. Solids* **55**, 327 (1994).
15. N. Frangis, S. Kuypers, C. Manolikas, J. van Landuyt, and S. Amelinckx, *Solid State Commun.* **69**, 817 (1989).
16. N. Frangis, S. Kuypers, C. Manolikas, G. van Tendeloo, J. van Landuyt, and S. Amelinckx, *J. Solid State Chem.* **84**, 314 (1990).
17. J. Horák, Z. Starý, P. Lošťák, and J. Pancíř, *J. Phys. Chem. Solids* **51**, 1353 (1990).
18. J. Horák, Z. Starý, and M. Matyáš, *J. Solid State Chem.* **93**, 485 (1991).